



Scientific-Research Article

# Darrieus Wind Turbine; Performance Enhancement Due to the Blade Cross-Section Optimization

Jafar Jafari<sup>1\*</sup>, Hamid Parhizkar<sup>2</sup>, Sadjad Ghasemlooy<sup>3</sup>

1-2-3- Department of Aerospace Engineering, Malek-Ashtar University of Technology, Tehran, Iran

## ABSTRACT

**Keywords:** Darrieus; VAWT; Aerodynamic Optimization; Shape Optimization; Simplex; Bezier Curve.

*This research investigates the effect of optimization of blade cross-section on the performance of the Darrieus wind turbine. The fluid flow around a Darrieus wind turbine is simulated by URANS (Unsteady Reynolds Averaged Navier Stokes) method. And blade cross-section was modeled by the Bezier curve and optimized to increase the average torque of the wind turbine. We used a novel, simple way for remeshing new design points in the optimization process. The Nelder-Mead simplex method was used for optimization, which enhanced the Turbine's performance by 33.7 percent. Results show that optimization of the blade cross-section is effective for increasing the performance of a VAWT (Vertical Axis Wind Turbine), and Nelder-Mead simplex is a proper and fast optimization method to be used in this case. Finally, the optimized airfoil was analyzed and compared with the initial one to understand optimization effects. It was concluded that optimization was more effective in azimuth positions of 90 to 160 degrees. And it decreased the performance in some regions according to changing nature of flow around each blade because of rotational motion. Analyzes show that optimization increased the Turbine's performance by increasing lift force of airfoil in some positions or affecting interaction flow - even accompanied by decreasing lift force of airfoil- in other positions, and it decreased performance in some other azimuth points.*

## Nomenclature

$A_S$ : Rotor projected area [ $m^2$ ]  
C: Airfoil cord length [m]  
 $C_P$ : Power coefficient [-]  
 $C_T$ : Torque coefficient [-]  
D: Drag force [N]  
 $D_{rotor}$ : Rotor diameter [m]  
 $F_n$ : Normal force [N]

$F_t$ : Tangential force [N]  
 $F_x$ : X-component force [N]  
 $F_y$ : Y-component force [N]  
 $H_{rotor}$ : Rotor height [m]  
k: Reduced frequency [-]  
L: lift force [N]  
n: Number of design variables [-]  
P: Mechanical power [W]  
R: Radial of rotating motion [m]

1 Msc. (Corresponding Author) Email: \* j\_jafari@outlook.com

2 Associate Professor

3 Assistant Professor

T: Torque [N.m]  
U: Relative velocity [m/s]  
 $U_A$ : Induced velocity [m/s]  
 $U_\infty$ : Free stream velocity [m/s]  
W: Incoming flow velocity [m/s]  
 $X_C$ : Contracted point [-]  
 $X_e$ : Expansion point [-]  
 $X_h$ : Most value point [-]  
 $X_r$ : Reflected point [-]  
 $\alpha$ : Angle of attack [rad]  
 $\rho$ : Air density [ $\text{kg/m}^3$ ]  
 $\lambda$ : Tip speed ratio [-]  
 $\theta$ : Azimuth position [deg]  
 $\omega$ : Rotational speed [rad/s]

#### Abbreviation

BEM: Blade Element Method  
CFD: Computational Fluid Dynamics  
HAWT: Horizontal Axis Wind Turbine  
LES: Large Eddy Simulation  
MDO: Multi-Disciplinary Optimization  
Simplex: Nelder-Mead simplex  
URANS: Unsteady Reynolds Averaged Navier-Stokes  
VAWT: Vertical Axis Wind Turbine

## Introduction

The increase of the human population and changes in lifestyles increase the energy demand every day. However, fossil energy resources are finite, and their harm to the environment is an essential restriction for using them. Thus human beings must utilize green energies (renewable energies) to survive, especially nowadays we confront the issue of global warming and the increase of CO<sub>2</sub> in the atmosphere. Optimizing engineering devices leads to reducing CO<sub>2</sub> emissions or gathering more green energies. Wind energy is free and accessible; it has been used since the olden days. Wind energy is mainly used through wind turbines which are made founded on windmills. Persian (Iranian) was the first to use windmills in 'Sistan' [1, 2]. These windmills -called "Asbad" in the local language- were made in 'Sistan' historical city, and people in other Iran's eastern parts have used them. Today, these windmills remain adjacent to Zabol city in Sistan-and-Baluchistan province, Iran. And some of these windmills are still working in Nashtifan city in Khorasan-Razavi Province, Iran.

Wind turbines are divided into two main groups. Horizontal Axis Wind Turbine (HAWT), blades rotate about an axis horizontal to wind direction. And Vertical Axis Wind Turbine (VAWT), in

VAWTs axis of rotation of blades is perpendicular to wind direction. VAWTs include Savonius and Darrieus turbines. In the Savonius turbine, blades are designed to create the most possible drag force, and this drag causes torque and so power. Therefore, Savonius turbine blades are like a semicircle, and this turbine is also called drag-driven VAWT. Darrieus turbines are known as lift-driven turbines, designed to catch wind energy by producing lift force in turbine blades. Since blades of the Darrieus turbine are supposed to produce lift force, they are airfoil shaped. The Darrieus turbines are straight bladed –also called H type- and eggbeater (also called  $\Phi$  type). The eggbeater is designed to reduce structural loads on blades, but it is more complex to manufacture and maintenance in comparison to a straight-bladed one. Hence straight bladed is the popular kind of Darrieus wind turbine. Darrieus wind turbines have the most efficiency among VAWTs. They are known for independence from wind direction, but they suffer from self-starting; however, Savonius wind turbines are suitable for self-starting.

A VAWT produces too low energy compared to a HAWT; because of that, HAWTs have fascinated researchers, and most research and applications of wind turbines are dedicated to HAWTs. However, in 2011 Dabiri [3] accomplished interesting research about wind farms. He compared the power in square meters produced by HAWTs and VAWTs. It was known that modern HAWTs have about  $2\text{-}3 \text{ Wm}^{-2}$  power density. He measured the power density of VAWTs experimentally, which was  $18 \text{ Wm}^{-2}$ , about 6-9 times HAWTs. He also estimated that the power density of VAWTs can get to  $30 \text{ Wm}^{-2}$  by using taller turbines.

Blade Element Momentum (BEM) methods are popular in rotational aerodynamic problems like propellers and horizontal axis wind turbines. The single streamtube model [4] is the first model to predict the performance of the Darrieus wind turbine. This model considers the whole rotor in a streamtube, so that rate of change of momentum in the streamtube represents forces applied on blades. Wilson and Lissaman [5] suggested Multi streamtube, which operates similarly to the single streamtube method. However, considering multi streamtubes instead of one, increases the precision. Muraca et al. [6] added some geometrical considerations like airfoil geometry and turbine solidity in multi streamtube model. Paraschivoiu [7] proposed a double multiple streamtube model,

which considers different induced velocities in actuator for windward and leeward regions. Other researches have progressed BEM models; more information is available in [8]. Streamtube models are invalid in high tip speed ratios and high rotor solidity; it ignores the velocity component normal to free velocity, solve the problem in a quasi-steady manner, and cannot simulate near-wake structures [9]. BEM methods are used to reduce the computational cost, which they are the best in.

Another numerical model for predicting the aerodynamic performance of VAWTs is the vortex model proposed by Larsen [10] In this model, blades are modeled by lifting lines. Strickland et al. [11] introduced a vortex model which determined flow domain in a dynamic manner – rather than quasi-steady- which facilitated simulation of a dynamic phenomenon. Other researchers have developed vortex models [12, 13, 14, 15], a detailed review of aerodynamic models is available in [8]. Vortex model is founded on potential flow, which considers irrotational inviscid flow, which is the main drawback of this model.

The BEM and Vortex models have a limiting requirement; before using them, aerodynamic data of blade cross-section is needed. There exist reliable references providing these data like [16, 17, 18]. However, the problem is that these data are gathered for airplane applications, so they do not contain Reynolds numbers and angles of attack that happen in Vertical Axis Wind Turbines (VAWT)s. [19] provides databases for only some airfoils in proper Reynolds numbers and angles of attack (0 to 180 degrees) for VAWTs. Evaluation of other airfoils using the BEM or Vortex model needs to determine aerodynamic data of the airfoil first, which causes computational or experimental costs.

Computational Fluid Dynamics (CFD) techniques are the most common methods to solve complex fluid dynamic problems, especially these days when we utilize powerful modern computers. The unsteady rotational flow domain of VAWTs can be simulated with a proper accuracy through URANS –Unsteady Reynolds Averaged Navier Stokes-methods. At the same time, the Direct Numerical Simulation (DNS) is not reasonable according to the enormous computational cost. Vassberg [20] was the first to use CFD tools to improve the design of VAWTs. Castelli et al. [21] proposed a new method using CFD to estimate the performance of the Darrieus wind turbine. CFD

methods have been deployed in VAWTs aerodynamic problems vastly, especially in recent works like Liang et al. [22] studied the performance of Darrieus-Savonius combined wind turbine. Akbar and Dabiri [23] used LES for studying the flow characteristics of the wake of VAWTs. There are many other researches about wind turbines and optimization like [24, 25, 26, 27]. According to the importance of VAWTs, there is some research about optimizing them. In 2015 Baz et al. [28] optimized the blades of the Savonius wind turbine. Kear et al. [29] optimized a VAWT using the Nelder-Mead simplex method in 2016. Moreover, Bedon et al. [30] in 2016 optimized the airfoil of a two-blade Darrieus wind turbine; they made airfoil shapes using the Bezier curve and utilized the Genetic Algorithm for optimization. However, they did not correctly deploy Bezier control points and the Genetic Algorithm. Improper use of Bezier control points led to 19 design variables for optimization. To reduce the computational cost –which became 3 months- they set 15 individuals and 5 generations in the optimization process, which cannot lead to convergence for 19 design variables. When optimization had not converged, the final point was not an optimum airfoil; it was a refined airfoil. Furthermore, it is not mentioned how much the average torque in a rotation (design function) was improved. Also, the final airfoil is an asymmetric airfoil; however, the Darrieus turbine is independent of wind direction. So the proposed airfoil is refined just for a specific wind direction. In this research, we employed Nelder-Mead simplex to optimize the airfoil of the Darrieus wind turbine and studied how it affects the turbine's performance. There are other parameters effective in the performance of the Darrieus wind turbine, such as: Tip Speed Ratio, rotor solidity, and wind velocity, which are considered constant to observe the effect of airfoil optimization lonely. We answered the following questions in this paper: How effective is Nelder-Mead simplex optimization in this case?

In which regions is optimization more beneficial?  
How does optimization improve the performance of the turbine?

Does optimization lead to decreasing the performance in any azimuth position?

## Methodology Principles

### Aerodynamic of Darrieus wind turbine

When an object subjected to incoming wind has a displacement vector, it is like the object is fixed and experiences two air flows: one in the direction of the incoming wind –with the velocity of wind– and the other in the reverse direction of displacement vector with the velocity of displacement, according to relative motion. Therefore, it experiences the airflow in the direction of the vector sum of incoming wind and reverse of the displacement. This changing in the direction of received airflow causes an angle of attack, which produces lift force in aerodynamic shapes like airfoils. In the Darrieus wind turbine, as shown in Figure 1, permanent displacement happens through rotational movement and makes  $\alpha$ , the angle of attack.

Figure 1 shows an airfoil rotating around an axis with the radius of  $R$ . This rotating motion causes an angle of attack just like a pitching airfoil. In Figure 1,  $U$  is defined by Eq. (1),  $U_\infty$  is the incoming wind and  $W$  is determined by Eq. (2) as below:

$$\vec{U} = -\vec{\omega} \times \vec{R} \quad (1)$$

$$\vec{W} = \vec{U}_\infty + \vec{U} \quad (2)$$

As Figure 1 shows geometrically,  $\alpha$  is calculated by Eq. (3):

$$\begin{aligned} \tan \alpha &= \frac{U_\infty \sin \theta}{U + U_\infty \cos \theta} \\ &= \frac{\sin \theta}{\frac{R\omega}{U_\infty} + \cos \theta} \xrightarrow{\text{yields}} \\ \alpha &= \tan^{-1} \frac{\sin \theta}{\lambda + \cos \theta} \end{aligned} \quad (3)$$

Such that  $\lambda$ , Tip Speed Ratio (TSR) is determined in Eq. (4) as the ratio of the speed of the blade's tip to incoming wind speed.

$$\lambda = \frac{R\omega}{U_\infty} \quad (4)$$

Eq. (3) defines the angle of attack for a rotating airfoil in Figure 1, which is like a pitching airfoil motion. In some researches [31, 32], The angle of attack in the Darrieus wind turbine is considered as in Eq. (3). In addition to this pitching effect, there is the interaction between vortexes-blades and between blade-blade in a Darrieus turbine. By considering vortex effects, the speed of wind encountering airfoil is not  $U_\infty$ , it is called  $U_A$ , and so  $\alpha$  is calculated by Eq. (5) in this circumstance.

$$\alpha = \tan^{-1} \frac{\sin \theta}{\lambda \frac{U_A}{U_\infty} + \cos \theta} \quad (5)$$

In part 0,

**Results and Discussions**, we considered the pitching effect of the airfoil to analyze the produced lift force by initial and optimized airfoils.

When airflow encounters the airfoil with an angle of attack, as in Figure 2, it makes Lift and Drag forces.

Aerodynamic forces in Figure 2 are decomposed into normal force ( $F_n$ ) and tangential force ( $F_t$ ). In Darrieus turbine  $F_t R$  represents the produced torque ( $T$ ). torque coefficient ( $C_T$ ) and power coefficient ( $C_P$ ) are determined by Eq. (6) and Eq. (7) respectively.

$$C_T = \frac{T}{\frac{1}{2} \rho A_S U_\infty^2} \quad (6)$$

$$C_P = \frac{P = T\omega}{\frac{1}{2} \rho A_S U_\infty^3} \quad (7)$$

While  $A_S$  is calculated by Eq. (8):

$$A_S = \frac{D_{rotor} \cdot H_{rotor}^{2D}}{A_S = D_{rotor}} \quad (8)$$

According to Eq. (6) and (7), torque is responsible for the turbine's performance. In this research, we considered the average torque in a complete rotation as the design function of the optimization process.

### Nelder-Mead simplex

Optimization methods can be classified into three major categories: Gradient Based Methods (GBM), Direct Search Methods and Stochastic Methods. These categories have different operating ways and thus different behaviors; one should know each well –advantages and disadvantages– and decide to select a method according to the problem.

In Gradient based methods, the gradient of the objective function is used to state the direction of searching for a new objective vector. The most used GBM is the adjoint method; many recent researches used Adjoint for optimization [33, 34, 35]. Adjoint methods are fast and have low computational cost, but they are case sensitive and must be developed whenever the problem changes, which means they are not robust. They also have develop-cost instead of their low computational cost. The development cost accompanies them with simplifying assumptions in some cases, which makes them improper for real engineering applications. GBMs are not supposed to survive from local optimum points because of the way they operate.

In direct search methods, the direction of searching for a new design vector is defined using the value of the objective function; hence the derivatives of the objective function are not needed, and direct search methods do not need a continuous design space as GBMs do. It facilitates direct search methods to treat the objective function as a black box, thus being a robust method. These methods are suitable for problems with a small number of variables [36]. Nelder-Mead simplex is the most popular direct search method. Direct search methods are robust but more computationally expensive than GBMs. They lead to local optimum most of the time, so they are better to be used in problems where optimum design and initial one are not too different. Stochastic methods -also called modern [36] or metaheuristic [37] methods- They are the most robust methods for optimization, they treat the objective function as a black box, and the number of design variables does not matter. These methods establish new design vectors upon stochastic operations and former design vectors. Thus, they can escape from local optimum points and often lead to global optimization. The main disadvantage of these methods is the high computational cost. Genetic Algorithm (GA), based on the theory of survival by Darwin and posed by Holland [38] for the first time- is the most popular stochastic method in engineering optimization.

In these problem we used Nelder-Mead simplex (simplex) [39], the most popular direct search method for optimization. A simplex is a simple geometry formed by  $n+1$  points, where  $n$  is the number of design objectives. For example, in a two dimensional problem, simplex is a triangle. In the simplex method for optimization, the initial simplex is formed according to the dimensions and starting point of the problem. Then simplex moves into the design space to lead optimum point. The movement of simplex happens through three operations: *Reflection*, *Expansion* and *Contraction*. These operations are explained below for a two dimensional minimizing problem.

In reflection operation, the point representing the most value of design function among simplex points ( $X_h$ ), is reflected to achieve a better point ( $X_r$ ). Figure 3 illustrates the reflection operation.

Now the new simplex is formed by a new point ( $X_r$ ). if  $X_r$  has the minimum value of objective function among points of new simplex, the

expansion operation occurs, as shown in Figure 4. Furthermore, if  $X_r$  has the maximum objective function value, contraction happens. Figure 4 illustrates expansion and contraction operations.

In Figure 4, the left side shape demonstrates expansion operation and the right side one, contraction operation. Finally, the simplex method for a minimizing problem is shown in Figure 5 as a flowchart.

### CFD Validation

In this research, we simulated the fluid domain around a Darrieus wind turbine. We used URANS (Unsteady Reynolds Averaged Navier Stokes) turbulence model in commercial CFD code ANSYS Fluent 16.1 for modelling unsteady turbulent and rotational flow field. The subsonic rotational flow around a WAVT needs to consider a large domain for simulation, so 3D simulation of such a domain is too computational cost, especially in optimization problems where we need to run the simulation many times. By ignoring 3D effects –mainly on the tip of blades- it is reasonable to simulate a VAWT in 2D, as some previous researches [21, 31, 30, 40, 41, 42, 28, 29]. We referred to Castelli et al. [21] research to validate CFD results, where both wind tunnel results and 2D CFD simulation were available. They simulated a three blade Darrieus wind turbine by NACA 0021 airfoil. Also, Mohamed [31] used this research for validation.

We considered a large domain, as shown in Figure 6, to ensure that it captures the wake development. Figure 6 also displays boundary conditions in the domain. The interface boundary condition separates the stator domain –the parts shown in Figure 6- and the rotary domain, which is indicated in Figure 7.

The numbers in Figure 6 and Figure 7 are in millimeters. We used a hybrid meshing, structured mesh in the boundary layer and Delaunay-loop-grid tri mesh in the rest of the domain. Figure 8 shows the hybridization of mesh in the trailing edge. And mesh in the interface of rotational and stationery domains is displayed in Figure 9.

A demanding part of aerodynamic shape optimization problems is to mesh a new domain as the new shape is constructed; this procedure takes more time in real engineering problems containing large and complicated domains. As Versteeg and Malalasekera stated: ‘‘Over 50% of the time spent in industry on a CFD project is devoted to the

definition of the domain geometry and grid generation'' [43]. An elegant solution is to deform the mesh to adapt to the new geometry. Gough [44] used the mesh morphing technic to deform mesh in optimization of Flow pass. Wang et al. [45] used a modern way instead of remeshing or deforming the mesh, and they adopted interior parameterization; The method is explained in [46]. The disadvantage of such methods is that they are limited to structure meshes, while actual engineering applications have complicated geometries which sometimes need unstructured or hybrid grids. Also, deforming a mesh has some constraints, as Gao [47] stated four. Keeping the quality of meshes does not let you deform the mesh as long as you wish, especially in viscous flows containing boundary layer mesh which are thin cells and can be damaged easily. Thus deforming mesh will prevent optimization to the global optimum point.

In this research, a novel, simple procedure is used to remesh only cells near the deforming walls using interior boundary conditions inside the solution domain. So it lets the optimization procedure lead to the global optimum while not needing to remesh the whole domain. It means that in every optimization loop, the mesh of the whole domain remains unchanged, but the mesh in the circle around each blade is represented by "interior" in Figure 7.

Relizable k-ε turbulent model [48] was used in this research, which is proper for rotational flow problems and has been used in many VAWT simulations [21, 31, 49, 50, 51, 52].

To estimate the wall  $Y^+$  on three blades, we calculated Area-Weighted Average over walls of three blades, which became 35.52 after modifying boundary layer meshes. Furthermore, it should be from 30 to 300 for using the Relizable k-ε turbulent model.

Reduced Frequency ( $k$ ) is a criterion for steadiness in flow field. It is defined by Eq. (9) for a rotating airfoil, and while  $k > 0.05$  the flow is unsteady [53].

$$k = \frac{\omega C}{2U} \quad (9)$$

For the Darrieus wind turbine Eq. (9) can be written in Eq. (10) form as below:

$$k = \frac{\omega C}{2U} \approx \frac{\omega C}{2R\omega} = \frac{C}{2R} \quad (10)$$

In this case  $k = 0.083$  therefore, we solved it in unsteady mode and used the Sliding Mesh Model for the rotational motion of blades.

The validation of the Whole CFD simulation is displayed below in Figure 10; in this validation, we observed Power Coefficient in 7 different TSRs from 1.4 to 3.3. In Figure 10, the current simulation results are placed between two primary 2D CFD researches [21, 31] and near to experimental results from wind tunnel tests [21].

We made many different meshes for this case to notice essential regions where higher amounts of gradients exist and should have finer grids. After all, the effect of the best mesh on simulation was estimated in different numbers of cells, as shown in Figure 11.

The mesh with 16000 cells was selected as proper mesh. As in Figure 11, when we increased the number of cells more than two times, the power coefficient changed by about 2.5 percent.

Finally, we set the time step size to  $3e-3$  second because, by this size, the convergence criteria for residuals ( $1e-5$ ) was met in almost all time steps. Moreover, when we halved the time step size to  $1.5e-3$  second, the power coefficient changed by less than 2 percent.

## Optimization

### Bezier Curve

Bezier curves are used to predict a smooth curve crossing particular points. They are used to characterize a shape by less number of variables. For example, an airfoil made from almost 100 points can be determined by less than ten control points in the Bezier curve. Bezier curves are defined by Eq. (11):

$$P(t) = \sum_{i=0}^n B_i J_{n,i}(t), \text{ Where:} \quad (11)$$

$$J_{n,i}(t) = \frac{n!}{i!(n-i)!} t^i (1-t)^{n-i}$$

While in Eq. (11),  $B_i$  are vertices of a Bezier polygon [54]. As the number of control points (vertices of a Bezier polygon) increases, the curve gets more accurate. [54] modeled a whole airfoil with 7 and 11 control points; they found that 11 control points were accurate enough.

In the case of the Darrieus wind turbine, the airfoil should be symmetric to form a wind direction independent turbine. Also, Mohamed [31] found

that symmetric airfoils are more efficient. So we modeled just a half of the airfoil by the Bezier curve, and we used 7 control points just for a half, as shown in Figure 12.

On the right side of Figure 12, NACA 0021 airfoil is modeled by 3 and 7 control points and compared with the original points of the airfoil. The picture is zoomed-in at the leading edge on the left side of Figure 12 ; it shows that the Bezier curve with 7 control points reasonably lies on the original airfoil points. We used Matlab code in [55] for modeling NACA 0021 airfoil by the Bezier curve as the initial point of the optimization process. Figure 13 shows a half of NACA 0021 modeled by the Bezier curve and the control points.

In Figure 13, control points are displayed by circles; the first is at the leading edge, and the last is at the trailing edge. Control points number 6, and 7 are so close to each other and hard to discrete in Figure 13. Each control point is determined by X and Y components, but changing the X component of control points does not change the curve significantly, and terminal control points cannot significantly affect the Bezier curve. So the X position of control points and terminal control points is usually considered constant in optimization problems like [56]. Thus, we considered Y components of central control points –shown by filled circles in Figure 13- as design variables in this optimization process.

### Optimization Framework

We made an optimization framework by Matlab Programming, as shown in Figure 14.

In Figure 14, the initial values of parameters are calculated by modeling NACA 0021 airfoil using Matlab code in [55]. The Y component of three central Control points for NACA 0021 are the initial values of three design variables. Then in each optimization loop, we made new airfoil points from Bezier control points using a code from [57].

A Gambit journal file reads new airfoil points and creates the new mesh. Using Gambit journal file facilitates unstructured and hybrid mesh schemes. Then, a journal file executes commands of ANSYS Fluent. Since the airflow around a Darrieus wind turbine is unsteady, [31] set 4 complete revolutions to analyze the flow, and we set 6 complete revolutions. The average torque in the last revolution is set as the design function.

Also, we used the Nelder-Mead simplex code arranged in Matlab R2016b as “fminsearch”.

## Results and Discussions

### Optimization Results

We optimized the airfoil of a Darrieus wind turbine by defining the airfoil through 3 design variables. The optimization method was Nelder-Mead simplex, and optimization was supposed to increase the average torque. Since the simplex method is a minimizing one, we defined the design function as the minus of average torque. In this optimization problem, we determined no physical constraints because the blades are supposed to produce lift force. The initial point of optimization is an airfoil; thus, we anticipated the optimum point to be another airfoil –not a very different shape- therefore no need for constraints. However, optimization procedures always check design points near the bounds of design variables (constraints). In a shape optimization problem, if the optimization procedure meets a design point, unable to be meshed and then solved, it may diverge. So we found out the values for design variables which led to damage to the blade shape and set them as optimization constraints. Thus the design variables X1 and X2 were bounded between 0.05 and 0.3 and X3 between 0.01 and 0.1. As shown in the below chart of Figure 15, optimization improved the average torque from 1.72 to 2.3 N.m, about 33.7 percent incensement. The above chart in Figure 15, displays the number of function evaluations in the optimization process, which is 125 times for the whole process. An increase of about 30 percent in a single Darrieus wind turbine performance is not a remarkable achievement in energy management. However, while considering a wind farm, this optimization provides a considerable increase in energy. Also, it should be noticed that a type of wind turbine will be used in more than one wind farm.

The initial point of optimization was NACA 0021; Figure 16 compares the initial and the final airfoil shapes. In Figure 16, the maximum thickness has increased, and its location is displaced too. The nodes of the new airfoil are provided in Appendix A.

The optimum airfoil has a greater area than the initial one; if the blades are producing filled, it

means an increase in the mass of blades. While the rotor's mass increases, the natural frequency will reduce, so the resonance phenomenon becomes more probable. A simple way to counter this and increase natural frequency is to change the dimensions and cross-section of arms, which connect blades to the central shaft. Another side effect of additional mass is an increase in rotational inertia of the rotor, which means more starting and brake torque for controlling the system. However, the blades of Darrieus wind turbines are not filled most of the time. Thus there will be no additional mass and side effects in many applications.

### Discussions

To analyze the optimization effects, we plotted instantaneous torque during the last revolution for one of the three blades of the turbine with both initial and optimized airfoils in Figure 17.

As shown in Figure 17, optimization was more beneficial in azimuth angles 90 to 160 degrees however it was injurious in some regions, and the worst part is between 184 to 215 degrees.

The Darrieus wind turbine is called lift driven turbine too, and the critical rule of an airfoil is to produce lift force which can be called airfoil efficiency. In 160-degree azimuth, as shown in Figure 18, there is a large separation region on the trailing edge of the initial airfoil. In contrast, in Figure 19, this region is reduced for the optimized airfoil, and the lift force is increased in the optimized airfoil. The streamlines in Figure 18 and Figure 19 are colored by velocity magnitude.

In 113-degree azimuth, the turbine performance was increased. However, the lift force of the airfoil was decreased. In Figure 20, the flow around the initial airfoil is attached to the airfoil (except in the trailing edge). However, in Figure 21, flow is separated from the optimized airfoil and forms a vortex region above it. So lift force is decreased in the optimized airfoil.

Figure 22 displays static pressure contour around the initial airfoil in 113-degree azimuth. Figure 22, a significant low-pressure region exists around the trailing edge, which causes an adverse pressure gradient and prevents rotational motion. However, the separated flow in Figure 21 decreases the low-pressure region in the optimized airfoil, as shown in Figure 23, and increases the turbine's performance. Finally, the optimization decreases turbine performance in azimuth of 184-degree

where the airfoil is located back to flow. As demonstrated in Figure 24, in 184-degree azimuth, a high-pressure region forms on the airfoil's leading edge, which makes an adverse pressure gradient. The high-pressure region of the optimized airfoil in Figure 25 is bigger than the one for the initial airfoil in Figure 24. This more prominent high-pressure region and so adverse pressure gradient in the optimized airfoil reduced the horizontal pressure force in the optimized airfoil  $-0.347$  N in the initial airfoil and  $0.042$  N in the optimized airfoil- and so the performance of the turbine.

### Calculating lift and drag forces

As we wanted to analyze the effect of optimization on the airfoil, it was challenging to calculate the lift and drag forces of a rotating airfoil in each time step. We used a UDF in ANSYS Fluent to obtain forces in X and Y directions –called  $F_x$  and  $F_y$ – on airfoil.

The tangential and normal forces of the airfoil ( $F_t$  and  $F_n$ ) with respect to  $F_x$  and  $F_y$  are displayed in Figure 26. In Figure 26,  $\theta$  is azimuthal position of the airfoil. According to Figure 26,  $F_t$  and  $F_n$  are determined by Eq. (12) and Eq. (13).

$$F_t = -F_x \cos \theta - F_y \sin \theta \quad (12)$$

$$F_n = F_x \sin \theta - F_y \cos \theta \quad (13)$$

Having  $F_t$ ,  $F_n$  and  $\alpha$ , lift and drag forces can be calculated as their connection is shown in Figure 2. Thus, lift and drag are concluded from Eq. (14) and Eq. (15):

$$L = F_t \sin \alpha + F_n \cos \alpha \quad (14)$$

$$D = -F_t \cos \alpha + F_n \sin \alpha \quad (15)$$

Finally, the instantaneous lift and drag force of the optimized turbine and initial turbine are compared in Figure 27 and Figure 28, respectively. In Figure 27 and Figure 28, lift and drag forces are calculated for one blade of each turbine in the last revolution.

The UDF for calculating lift and drag forces is embedded in Appendix B, and Appendix C explains how to link the commercial software and make a framework.

### Conclusions

We used Nelder-Mead simplex for optimizing the airfoil of a Darrieus wind turbine. The optimization led to an increase in the average



torque of about 33.7 percent. This research had the below findings:

The Nelder-Mead simplex is a proper and fast optimization method for optimizing a VAWT blade cross section.

Optimization of the blade cross-section is helpful for increasing the performance of a VAWT.

Optimization was more effective in azimuth positions of 90 to 160 degrees. Moreover, it decreased the performance in some regions according to changing nature of flow around each blade because of rotational motion.

The optimization increased the turbine performance by increasing the lift force of the airfoil or affecting interaction flow (even accompanied by decreasing lift force of the airfoil). Moreover, it decreased performance in some azimuth positions.

In this research, we observed the effect of the rotor cross-section on the turbine's performance. For future studies, we suggest Multi-Disciplinary Optimization (MDO), which contains different rotor solidities and TSRs and cross-section changing. We also suggest optimization for 3D rotor geometry to study and improve 3D aerodynamic phenomena in a VAWT rotor. Using more accurate turbulence methods like LES and considering aerodynamic noise in optimization are important issues for future studies.

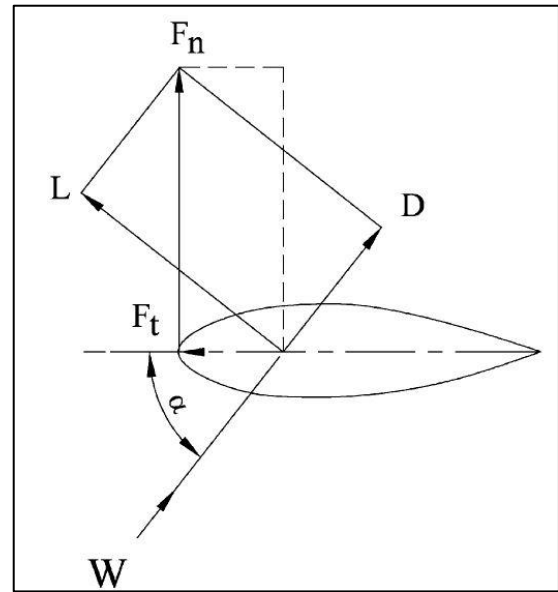


Figure 2 Lift and Drag forces.

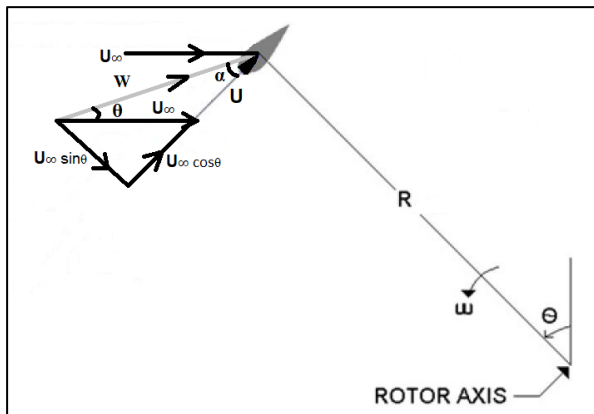


Figure 1 Angle of attack

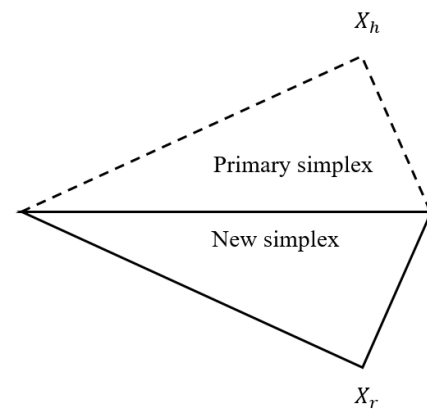


Figure 3 Reflection operation

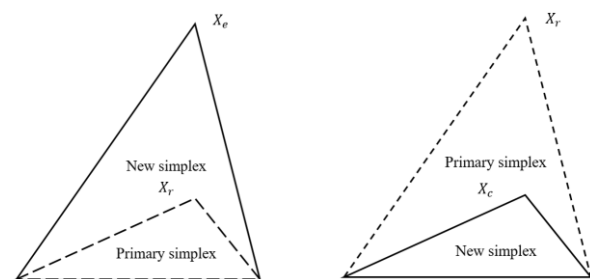


Figure 4 Expansion and Contraction operations

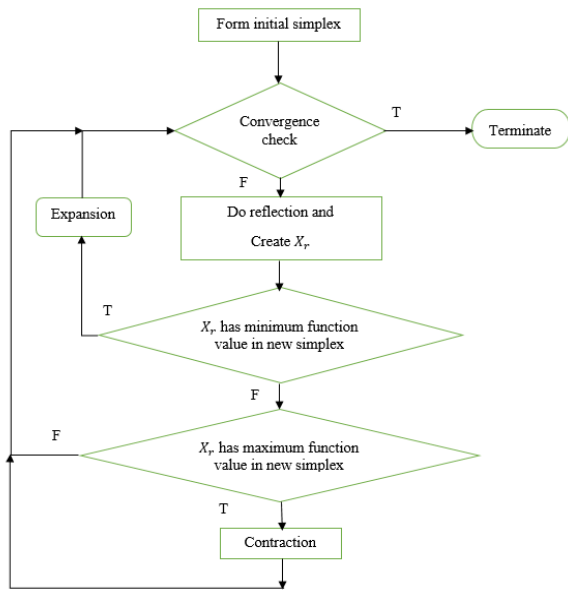


Figure 5 Flowchart of simplex method.

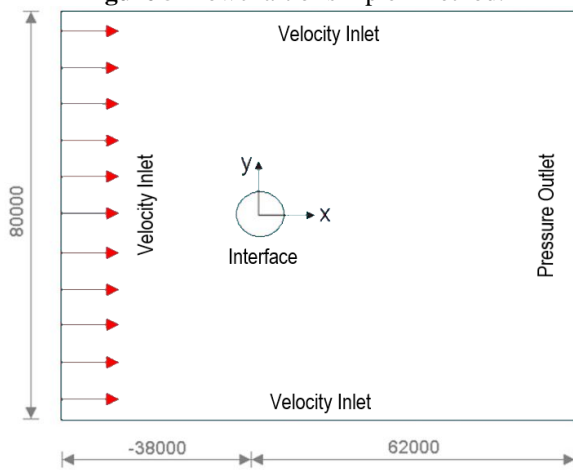


Figure 6 Dimensions of fluid domain.

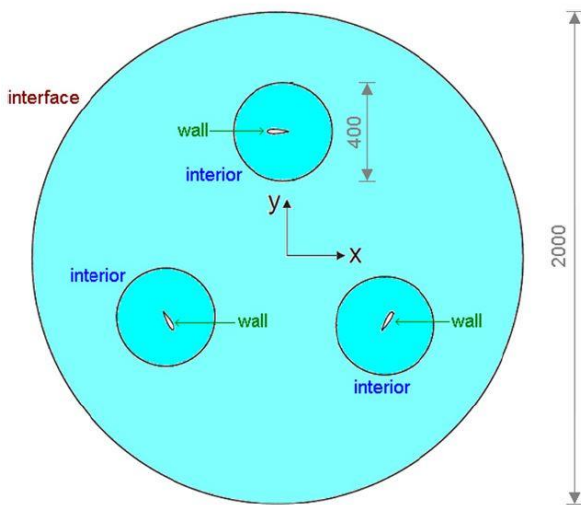


Figure 7 Rotary domain [21].

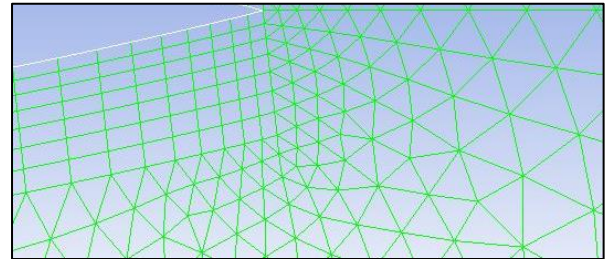


Figure 8 Hybrid mesh in trailing edge.

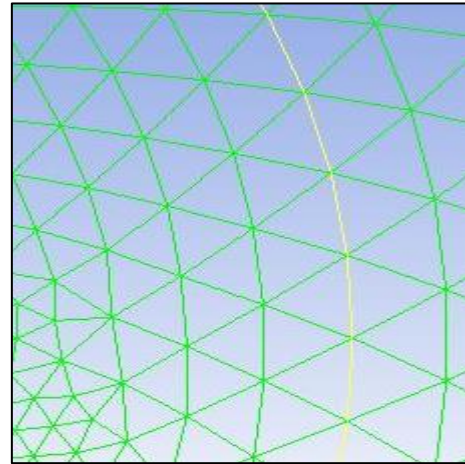


Figure 9 Mesh in interface region.

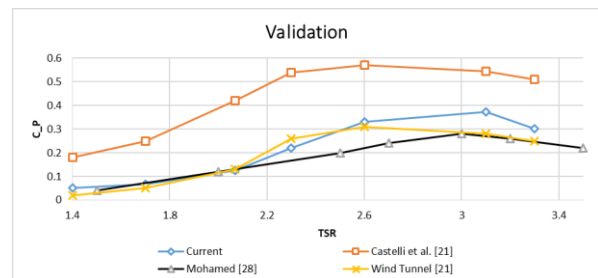


Figure 10 Validation.

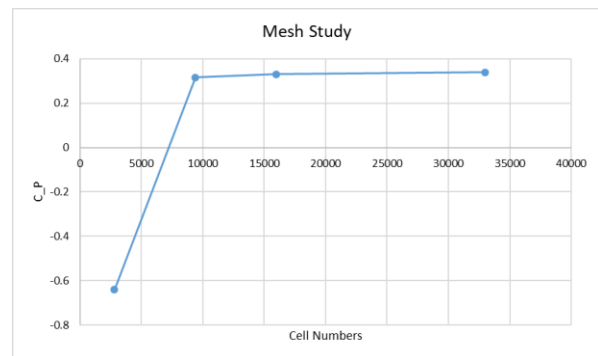


Figure 11 Mesh study.

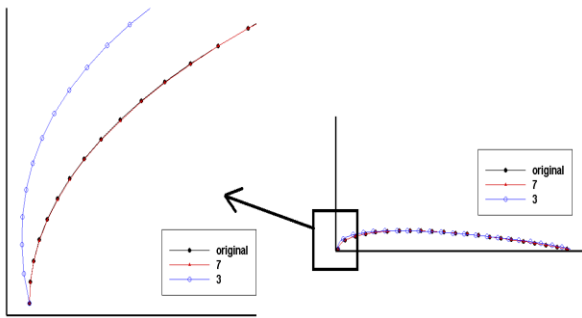


Figure 12 airfoil modelled by Bezier curve

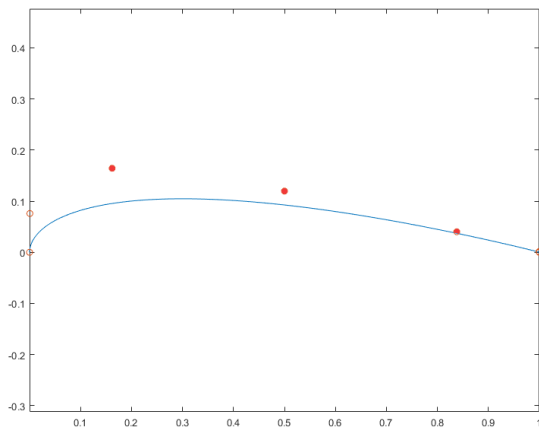


Figure 13 Half of NACA 0021 by Bezier curve

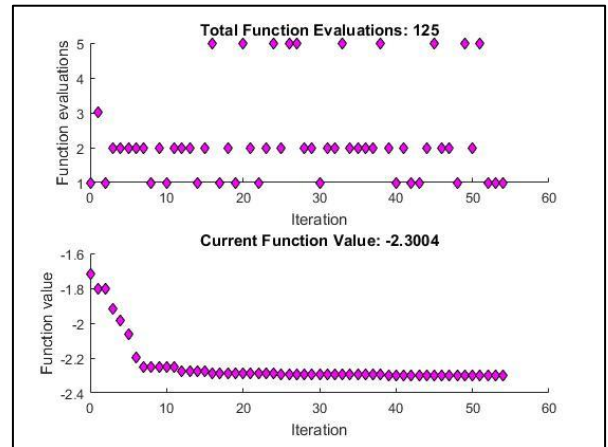


Figure 15 Optimization history.

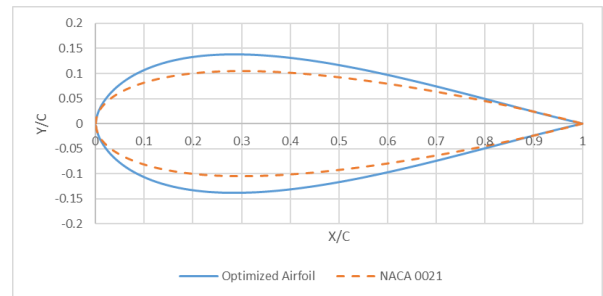


Figure 16 Initial and Final airfoils

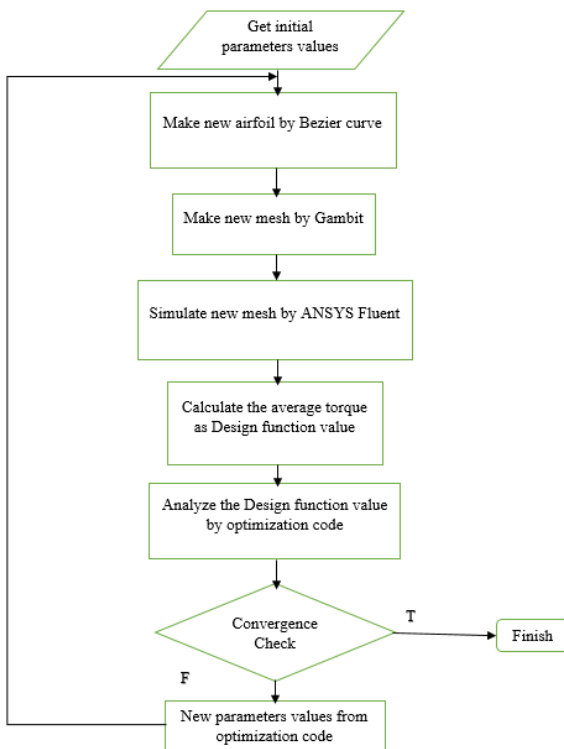


Figure 14 Flowchart of optimization framework

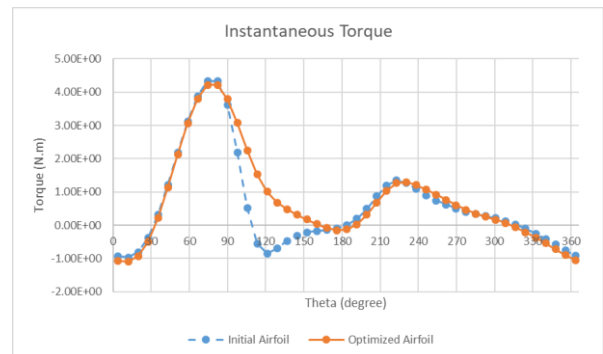


Figure 17 Instantaneous Torque

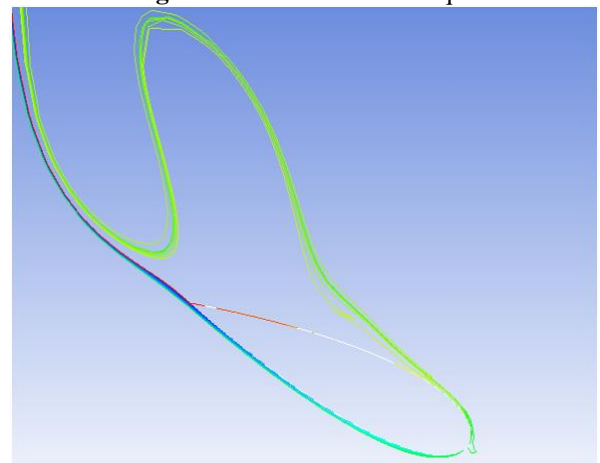


Figure 18 Streamlines of initial airfoil in 160-degree

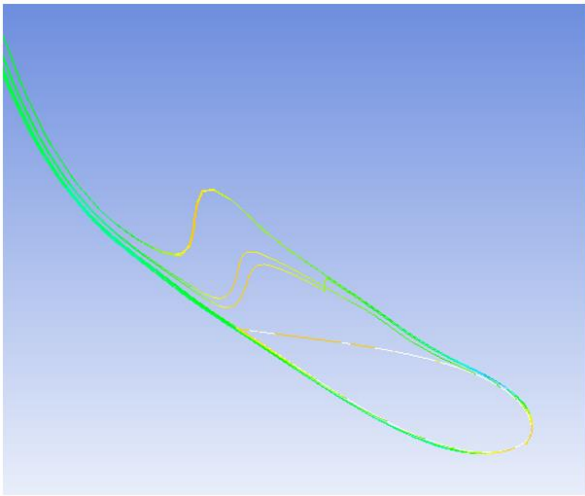


Figure 19 Streamlines of optimized airfoil in 160-degree.

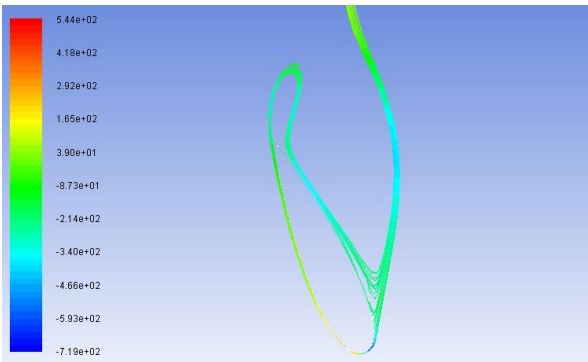


Figure 20 Streamlines of initial airfoil in 113-degree

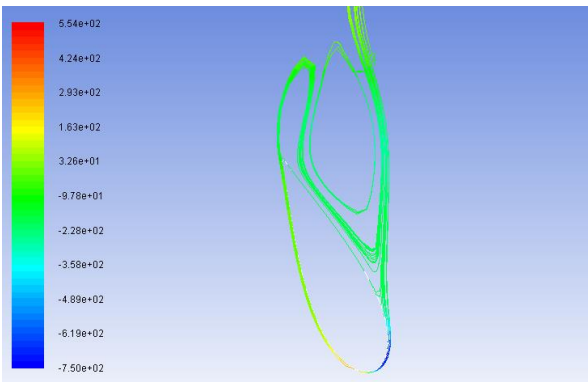


Figure 21 Streamlines of optimized airfoil in 113-degree

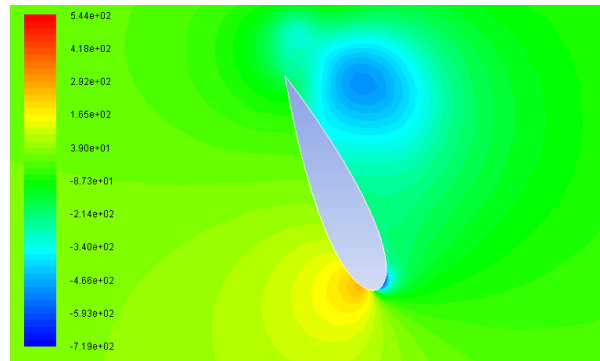


Figure 22 Static pressure contour of initial airfoil in 113-degree.

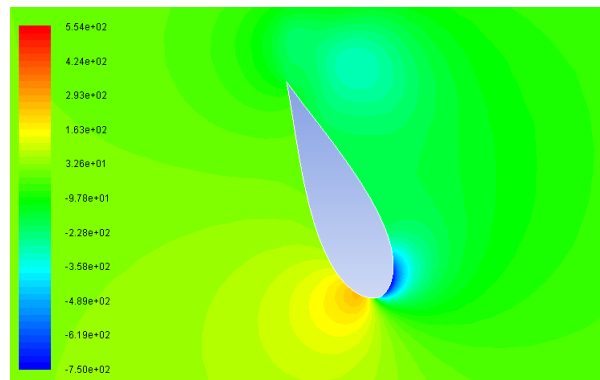


Figure 23 Static pressure contour of optimized airfoil in 113-degree

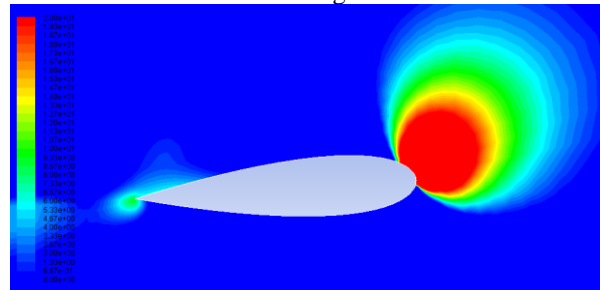


Figure 24 Static pressure contour of initial airfoil in 184-degree

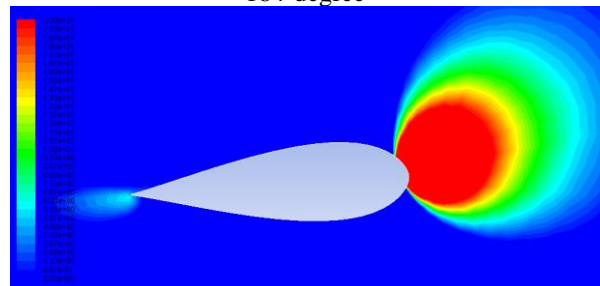


Figure 25 Static pressure contour of optimized airfoil in 184-degree

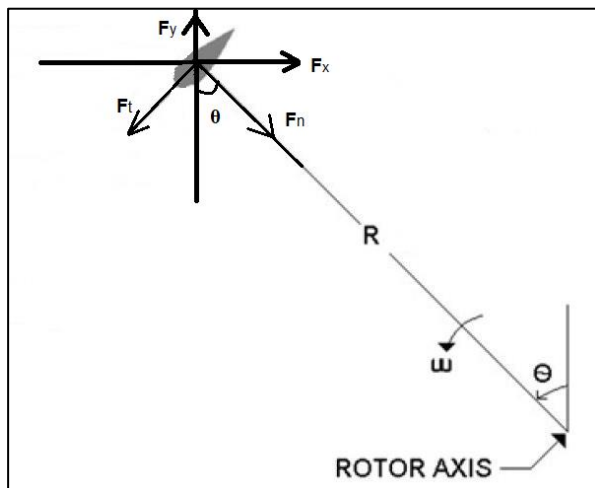


Figure 26 Forces of a rotating airfoil

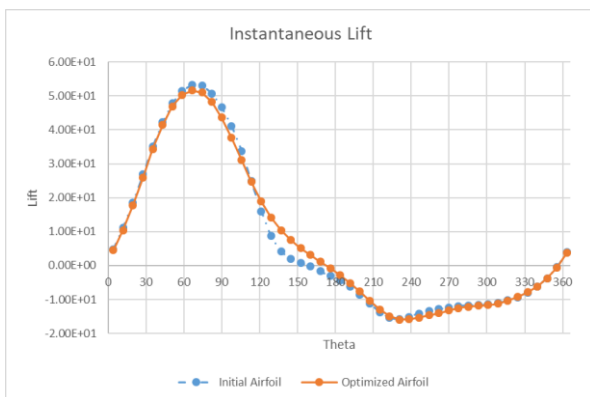


Figure 27 Comparison of Instantaneous Lift

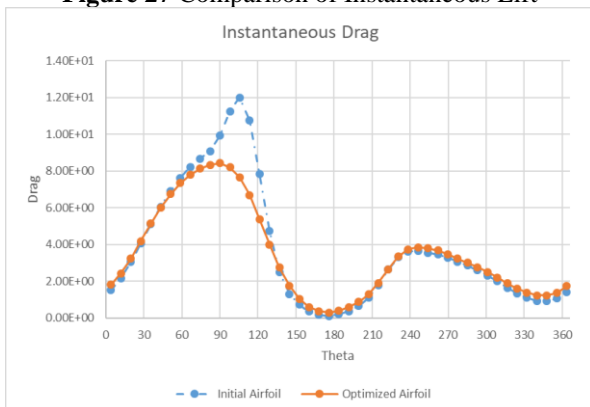


Figure 28 Comparison of Instantaneous Drag

## References

- [1] D. A. Spera, Wind Turbine Technology: Fundamental Concepts of Wind Turbine Engineering; Second Edition, New York: ASME PRESS, 2009.
- [2] "United Nations Educational, Scientific and Cultural Organization," 2 February 2017. [Online]. Available: <https://whc.unesco.org/en/tentativelists/6192/>. [Accessed 20 September 2019].
- [3] J. O. Dabiri, "Potential order-of-magnitude enhancement of wind farm power density via counter-rotating vertical-axis wind turbine arrays," *Journal of Renewable and Sustainable Energy*, vol. 3, 2011.
- [4] R. Templin, "Aerodynamic performance theory for the NRC vertical-axis wind turbine," NRC Lab., 1974.
- [5] R. Wilson and P. Lissaman, Applied aerodynamics of wind power machines, Oregon State University, 1974.
- [6] R. Muraca, M. Stephens and J. Dagenhart, "Theoretical performance of cross-wind axis turbines with results for a catenary vertical axis configuration," NASA, 1975.
- [7] Paraschivoiu, "Double-multi streamtube model for darrieus wind turbines," in *Second DOE/NASA wind turbines dynamics workshop*, Cleveland, 1981.
- [8] M. Islam, D. Ting and A. Fartaj, "Aerodynamic models for Darrieus-type straight-bladed vertical axis wind turbines," *Renewable and Sustainable Energy Reviews*, vol. 12, no. 4, pp. 1087-1109, 2008.
- [9] Paraschivoiu, Wind Turbine Design With Emphasis on Darrieus Concept, Polytechnic International Press, 2002.
- [10] H. Larsen, "Summary of a vortex theory for the cyclogiro," in *Proceedings of the second US national conferences on wind engineering research*, Colorado state, 1975.
- [11] J. Strickland, B. Webster and T. Nguyen, "A Vortex model of the darrieus turbine: an analytical and experimental study," Technical report SAND81-7017, Sandia National Laboratory, 1981.
- [12] J. Strickland, B. Webster and T. Nguyen, "Vortex model of the darrieus turbine: an analytical and experimental study," *American Society of Mechanical Engineers*.
- [13] J. Cardona, "Flow curvature and dynamic stall simulated with an aerodynamic free vortex model for VAWT," *Wind Engineering*, vol. 43, pp. 8-135, 1984.
- [14] P. Migliore, W. Wolfe and J. Fanucci, "Flow curvature effects on Darrieus turbine blade aerodynamics," *Energy*, vol. 4, no. 2, pp. 49-55, 1980.
- [15] N. Pawsey, *Development and evaluation of passive variable-pitch vertical axis wind turbines.*, Doctoral thesis, The University of New South Wales, 2002.
- [16] Abbott, Theory of Wing Sections: Including a Summary of Airfoil Data, New York: Dover Publications, INC., 1959.

- [14] F. W. RIEGELS, AEROFOIL SECTIONS, London: BUTTERWORTHS, 1961.
- [15] R. Eppler, Airfoil Design and Data, New York: Springer-Verlag Berlin Heidelberg, 1990.
- [16] R. Sheldahl and P. Klimas, Aerodynamic characteristics of seven symmetrical airfoil sections through 180-degree angle of attack for use in aerodynamic analysis of vertical axis wind turbines, SAND, 1980.
- [17] J. C. Vassberg, A. K. Gopinath and A. Jameson, "Revising the vertical-axis wind-turbine design using advanced computational fluid dynamics," *AIAA Paper, 43rd AIAA ASM*, 2005.
- [18] M. R. Castelli, A. Engaro and E. Benini, "The Darrieus wind turbine: Proposal for a new performance prediction model based on CFD," *Energy*, vol. 36, pp. 4919-4934, 2011.
- [19] X. Liang, S. FU, B. OU, C. WU and C. YH, "A computational Study of the Effect of the Radius and Attachment Angle on the Performance of a Darrieus-Savonius Combined Wind Turbine," *Renewable Energy*, no. doi: 10.1016/j.renene.2017.04.071, 2017.
- [20] M. Akbar and J. O. Dabiri, "Self-similarity and flow characteristics of vertical-axis wind turbine wakes: an LES study," *Journal of Turbulence*, vol. 18, no. 4, pp. 373-389, 2017.
- [21] M. Aziz and A. Jahangirian, "Aerodynamic Optimization of a Wind Turbine Blade for Maximum Annual Energy Production at Manjil Wind Farm," *Journal of Aerospace Science and Technology*, vol. 14, no. 2, pp. 1-9, 2021.
- [22] M. Fakoor, S. Ghoreishi and M. Aminjafari, "Multi-objective Optimization of Buckling Load for a Laminated Composite Plate by Coupling Genetic Algorithm and FEM," *Journal of Aerospace Science and Technology*, vol. 12, no. 1, pp. 27-36, 2019.
- A. N. S. Astaraki, "Optimization of Sound Transmission Loss of a Composite Rectangular Plate with Infinite Baffle," *Journal of Aerospace Science and Technology*, vol. 11, no. 2, pp. 43-51, 2017.
- [23] M. Fakoor, P. Mohammadzade and E. Jafari, "Optimization of Composite Stiffened Cylindrical Shell using PSO Algorithm," *Journal of Aerospace Science and Technology*, vol. 11, no. 2, pp. 43-51, 2017.
- A. M. Baz, N. A. Mahmoud, A. M. Hamed and K. M. Youssef, "Optimization of two and three rotor savonius wind turbine," in *Proceeding of ASME Turbo Expo 2015: Turbine Technical Conference and Exposition*, Montreal, 2015.
- [24] M. Kear, B. Evans, R. Ellis and S. Rolland, "Computational Aerodynamic Optimization of Vertical Axis Wind Turbine Blades," *Applied Mathematical Modeling*, no. doi: 10.1016/j.apm.2015.07.001, pp. 1-18, 2015.
- [25] G. Bedon, S. D. Betta and E. Benini, "Performance-optimized airfoil for Darrieus wind turbines," *Renewable Energy*, vol. 94, pp. 328-340, 2016.
- [26] M. Mohamed, "Performance investigation of H-rotor Darrieus turbine with new airfoil shapes," *Energy*, vol. 47, pp. 522-530, 2012.
- [27] Z. Zhao, R. Wang, W. Shen, T. Wang, B. Xu, Y. Zheng and S. Qian, "Variable Pitch Approach for Performance Improving of Straight-Bladed VAWT at Rated Tip Speed Ratio," *Applied Sciences*, vol. 8, no. doi:10.3390/app8060957, 2018.
- [28] C. B. Dilgen, S. B. Dilgen, D. R. Fuhrman, O. Sigmund and B. S. Lazarov, "Topology optimization of turbulent flows," *Computer Methods in Applied Mechanics and Engineering*, vol. 331, pp. 363-393, 2018.
- [29] K. Wang, S. Yu, Z. Wang, R. Feng and T. Liu, "Adjoint-based airfoil optimization with adaptive isogeometric discontinuous Galerkin method," *Computer Methods in Applied Mechanics and Engineering*, vol. 344, pp. 602-625, 2019.
- [30] E. M. Papoutsis-Kiachagias, S. A. Kyriacou and K. C. Giannakoglou, "The continuous adjoint method for the design of hydraulic turbomachines," *Computer Methods in Applied Mechanics and Engineering*, vol. 278, pp. 621-639, 2014.
- [31] S. S. Rao, *Engineering Optimization Theory and Practice*, Fourth Edition, John Wiley & Sons, Inc., 2009.
- [32] S. Sivanandam and S. N. Deepa, *Introduction to Genetic Algorithms*, Springer, 2002.
- [33] J. H. Holland, *Adaptation in Natural and Artificial System*, Michigan: University of Michigan, 1975.
- [34] J. A. Nelder and R. Mead, "A simplex method for function minimization," *J. Comput.*, vol. 7, pp. 308-313, 1965.

- I. Hashem and M. Mohamed, "Aerodynamic Performance Enhancement of H-rotor Darrieus Wind Turbine," *Energy*, no. doi: 10.1016/j.energy.2017.10.036, 2017.
- [35] M. Mohamed, A. Dessoky and F. Alqurashi, "Blade shape effect on the behavior of the H-rotor Darrieus wind turbine: Performance investigation and force analysis," *Energy*, vol. 179, pp. 1217-1234, 2019.
- [36] Y. Wang, S. Shen, G. Li, D. Huang and Z. Zheng, "Investigation on Aerodynamic Performance of Vertical Axis Wind Turbine with Different Series Airfoil Shapes," *Renewable Energy*, no. doi: 10.1016/j.renene.2018.02.095, 2018.
- [37] H. K. Versteeg and W. Malalasekera, *An Introduction to Computational Fluid Dynamics The Finite Volume Method*, Harlow: Pearson Educational Limited, 2007.
- [38] W. D. Gough, *Automated Flow Path Design Optimization Using Mesh Morphing. Master of Science Thesis*, Provo: Brigham Young University, 2011.
- [39] K. Wang, S. Yu, Z. Wang, R. Feng and T. Liu, "Adjoint-based airfoil optimization with adaptive isogeometric discontinuous Galerkin method," *Computer Methods in Applied Mechanics and Engineering*, 2018.
- [40] G. Xu, B. Mourrain, R. Duvigneau and A. Galligo, "Parameterization of computational domain in isogeometric analysis: methods and comparison," *Computer Methods in Applied Mechanics and Engineering*, Vols. 23-24, no. 200, pp. 2021-2031, 2011.
- [41] X. W. Gao, P. C. Chen and L. Tang, "Deforming Mesh for Computational Aeroelasticity Using a Nonlinear Elastic Boundary Element Method," *AIAA Journal*, vol. 40, no. 8, pp. 1512-1517, 2002.
- [42] T. Shih, W. Liou, A. Shabbir, Z. Yang and J. Zhu, "A new  $k-\epsilon$  eddy viscosity model for high Reynolds number turbulent flows," *Computers and Fluids*, vol. 24, no. 3, 1995.
- [43] M. Mohamed, G. Janiga, E. Pap and D. Thévenin, "Optimization of Savonius turbines using an obstacle shielding the returning blade," *Renewable Energy*, vol. 35, no. 11, 2010.
- [44] M. Mohamed, G. Janiga, E. Pap and D. Thévenin, "Optimal blade shape of a modified Savonius turbine using an obstacle shielding the returning blade," *Energy*, vol. 52, no. 1, 2011.
- [45] M. Moahamed, G. Janiga, E. Pap and D. Thévenin, "Multi-objective optimization of the airfoil shape of wells turbine used for wave energy conversion," *Energy*, vol. 36, no. 1, 2011.
- [46] R. Howell, N. Qin, J. Edwards and N. Durrani, "Wind tunnel and numerical study of a small vertical axis wind turbine," *Renewable Energy*, vol. 35, pp. 412-422, 2010.
- [47] J. G. Leishman, *Principles of Helicopter Aerodynamics*, second edition, Cambridge: Cambridge university Press, 2006.
- [48] F. Mohebbi and M. Sellier, "Aerodynamic Optimal Shape Design Based on Body-Fitted Grid Generation," *Mathematical Problems in Engineering*, no. <http://dx.doi.org/10.1155/2014/505372>, 2014.
- [49] F. Mohebbi, *Optimal shape design based on body-fitted grid generation*, New Zeland: PhD Thesis in Mechanical Engineering at the University of Canterbury, 2014.
- [50] D. Zing, M. Nemeč and T. Pulliam, "A comparative evaluation of genetic and gradient-based algorithms applied to aerodynamic optimization," *Shape design in aerodynamics*, pp. 103-126, 2008.
- [51] M. E. N. A. I. Ibrahim Zeid, "Mathworks," [Online]. Available: <https://www.mathworks.com/matlabcentral/fileexchange/12414-bezier-curve>.

**Appendix A.**

In this appendix, we put the points of the optimized airfoil to be used in the Darrieus wind turbine.

Since the airfoil is symmetric, we just put 100 points of the above halve in Table 1.

Table 1 Points of optimized airfoil.

	X	Y		X	Y		X	Y		X	Y
1	0	0	26	0.146449	0.123093	51	0.500002	0.116978	76	0.853559	0.035648
2	0.000279	0.00471	27	0.157731	0.12584	52	0.515703	0.114182	77	0.864492	0.03286
3	0.001041	0.0097	28	0.169352	0.128318	53	0.531388	0.111127	78	0.875066	0.030171
4	0.002288	0.014923	29	0.1813	0.130524	54	0.547043	0.108254	79	0.885268	0.027584
5	0.00402	0.020335	30	0.193562	0.132458	55	0.562651	0.105145	80	0.89509	0.025105
6	0.006236	0.025894	31	0.206127	0.134119	56	0.578198	0.101951	81	0.90452	0.022737
7	0.008936	0.03156	32	0.218981	0.13551	57	0.593668	0.098686	82	0.913551	0.020482
8	0.012118	0.037297	33	0.232113	0.136631	58	0.609046	0.095357	83	0.922172	0.018343
9	0.015778	0.043071	34	0.245508	0.137485	59	0.624317	0.091977	84	0.930375	0.016323
10	0.019916	0.048849	35	0.259155	0.138076	60	0.639466	0.088555	85	0.938153	0.014423
11	0.024526	0.0546	36	0.273038	0.138409	61	0.654477	0.085101	86	0.945497	0.012644
12	0.029605	0.060298	37	0.287146	0.138488	62	0.669337	0.081625	87	0.9524	0.010988
13	0.035149	0.065915	38	0.301462	0.138318	63	0.68403	0.078137	88	0.958856	0.009454
14	0.041151	0.071428	39	0.315974	0.137907	64	0.698543	0.074646	89	0.964859	0.008042
15	0.047608	0.076814	40	0.330668	0.13726	65	0.712859	0.071162	90	0.970402	0.006753
16	0.054511	0.082053	41	0.345527	0.136385	66	0.726967	0.067694	91	0.975481	0.005584
17	0.061855	0.087128	42	0.360539	0.13529	67	0.740851	0.06425	92	0.980091	0.004535
18	0.069633	0.09202	43	0.375687	0.133982	68	0.754497	0.060839	93	0.984228	0.003603
19	0.077836	0.096714	44	0.390958	0.132471	69	0.767893	0.057469	94	0.987888	0.002786
20	0.086457	0.101198	45	0.406336	0.130766	70	0.781025	0.054148	95	0.991069	0.002081
21	0.095488	0.105458	46	0.421806	0.128875	71	0.79388	0.050884	96	0.993768	0.001485
22	0.104918	0.109485	47	0.437353	0.126808	72	0.806444	0.047683	97	0.995984	0.000995
23	0.114739	0.11327	48	0.452961	0.124574	73	0.818707	0.044553	98	0.997715	0.000606
24	0.124942	0.116803	49	0.468616	0.122185	74	0.830654	0.0415	99	0.998961	0.000314
25	0.135515	0.120079	50	0.484301	0.11965	75	0.842276	0.038529	100	0.999723	0.000114

**Appendix B.**

In this appendix, we put the UDF we used for calculating lift and drag forces on a blade cross-section.

```
#include "udf.h"
/* this udf calculates Lift and Drag forces */
/* for a Rotating blade in each time step */
DEFINE_EXECUTE_AT_END(press)
{
Domain *domain = Get_Domain(1);
int ID = 72; /* the ID of required wall boundary condition */
real flow_time, m, tet, al, ft, fn, li, dr;
Thread *t = Lookup_Thread(domain, ID);
real CG[2], force[2], moment[3];
NV_S(CG, =, 0.0);
```

Compute\_Force\_And\_Moment(domain, t, CG, force, moment, TRUE);

```
/* By using this command we have forces in direction of */
/* Global X (force[0]) and Y (force[1]) */
flow_time = CURRENT_TIME;
/* Finding the Azimuth Angle (tet) and the Angle of Attack (al) */
tet = flow_time*45.437; /* Omega = 45.437 */
m = sin(tet)/(2.6 + cos(tet)); /* tsr = 2.6 */
al = atan(m);
/* Finding Tangential and Normal Forces */
ft = -force[0]*cos(tet) - force[1]*sin(tet);
fn = force[0]*sin(tet) - force[1]*cos(tet);
/* Finding Lift and Drag Forces */
li = ft*sin(al) + fn*cos(al);
```



```
dr = -ft*cos(al) + fn*sin(al);  
Message("(%e, %e)\n", li, dr);  
}
```

### Appendix C.

In this appendix, we explain the note-based method used to link ANSYS Fluent and Gambit with Matlab in Windows.

First, you should write a journal file for Gambit, which must include saving the new mesh file. As an example, save it as “mesh.msh”. Save the journal file in “.jou” format; for example, name it as “g.jou”. Then create a bat file in Windows Environment like “g.bat” this bat file contains three lines as below:

```
del default_id.dbs  
del mesh.loc  
C:\.....\gambit.exe -inp E:\.....\g.jou
```

Two first lines above are needed for the procedure to be repeated. In the third line, write the address of Gambit software on your PC in the first dotted place and the address of the Gambit Journal file into the second one. In the same manner, save the journal file of fluent as “f.jou”; for example, this journal must include reading “mesh.msh” and writing the design parameter-torque in this research- in a text file like “t.dat”. Then create a bat file named something like “f.bat”, which contains two lines like below:

```
del t.dat  
Fluent 2d -hidden -i E:\.....\f.jou
```

The first line above deletes the previous output so the new one can be written. And the second line runs ANSYS Fluent without GUI, which saves time in an optimization procedure.

In your Matlab code you can run these bat files easily, for example for “g.bat” write:

```
! g.bat
```

And so on.

---

#### COPYRIGHTS

©2023 by the authors. Published by Iranian Aerospace Society This article is an open access article distributed under the terms and conditions of the Creative Commons Attribution 4.0 International (CC BY 4.0)

<https://creativecommons.org/licenses/by/4.0/>.

